Drift Waves and Test Particle Transport in a Stellarator

A. Kendl, H. Wobig

Max-Planck-Institut für Plasmaphysik, EURATOM Association, D-85748 Garching bei München, Germany

1. Introduction

Electrostatic drift waves are a major candidate to cause anomalous transport in toroidal devices. In assessing the effect of drift waves on particle orbits one must distinguish between circulating particles travelling around the torus and trapped particles localised in magnetic mirrors. The present paper deals with circulating particles in stellarators and computes the orbits in guiding center approximation. Because of the small gyro radii drift surfaces and magnetic surfaces differ only little and the drift rotational transform is close to the magnetic rotational transform. Islands of magnetic surfaces will also lead to corresponding islands of drift surfaces. The parallel electric field of the drift surfaces modifies the energy of the particles, which introduces the effect of Arnold diffusion [1] as the combined effect of drift islands and time-varying electromagnetic fields. Recently J.M. Kwon et al.[2] have investigated the effect of drift waves on circulating particles in tokamaks using the mapping technique. Since the authors assume energy conservation particle orbits can be described by two coupled equations of an area preserving map. However, violation of energy conservation by time-varying electric field destroys this property and leads to four coupled equations [3]. In the following we follow this line and develop a set of mapping equations describing circulating particles in a Helias configuration [4]. Nonlinear drift waves in Helias configurations have been computed applying the turbulence code of B. Scott [5].

2. The model

Guiding center orbits in toroidal geometry can be described in terms of Hamiltonian mechanics in a 4-dimensional phase space. Reduction to 4 canonical variables has been discussed by Meiss and Hazeltine [6], who showed that a canonical coordinate system can be found where the covariant B_r -component can be eleminated by a proper choice of the angular coordinates. Neglecting the magnetic part of the drift waves leads to a time-independent coordinate system, otherwise the canonical coordinate system is time-dependent (see ref. 3). The Hamiltionian H_0+H_1 can be written in the form

$$H_0 = \frac{m}{2}u^2(p_\theta, p_\varphi, \theta, \varphi) + \mu B + q\Phi_0 \quad ; \quad H_1 = \delta h + q\delta\Phi$$
 Eq. 1

u is the parallel velocity, μ is the magnetic moment. The poloidal canonical momentum p_{θ} is roughly proportional to the radial coordinate r if the poloidal magnetic field is small compared with the toroidal one. The time-dependent part of the electric potential $\delta\Phi$ is the effect of the electrostatic drift waves, which in the following will be considered as a small perturbation. δh is the time-independent perturbation, which causes islands of the drift surfaces. The four canonical equations can be written in conjugate variables $p_{\theta}, p_{\varphi}, \theta$ and φ . However, in case of circulating particles the toroidal velocity is not zero, which allows one to introduce the energy E and the time t as conjugate variables and use the toroidal angle φ as the independent variable. To do so we invert the Hamiltonian and write the toroidal momentum p_{φ} as function of energy E and the other variables $p_{\varphi} = -K(E,t,p_{\theta},\theta,\varphi)$, which defines a new Hamiltonian K. Since the time-dependent term in Eq. 1 is small we obtain the following approximation of the new Hamiltonian

$$K = K_0 \Big(p_\theta, \theta, E, \varphi \Big) + K_1 \Big(p_\theta, \theta, E, t, \varphi \Big) \; \; ; \; \; K_1 = \frac{q \delta \Phi}{H_0' \Big(p_\varphi \Big)}$$
 Eq. 2

 K_0 is defined by $E = H_0(p_\theta, \theta, p_\phi = -K_0, \varphi)$. The denominator in the perturbation K_1 is the toroidal angular velocity of the particles, which shows that fast particles are less affected by the electrostatic waves than slow particles. The unperturbed Hamiltonian K_0 describes unperturbed drift surfaces characterised by the two "frequencies"

$$\iota(p_{\theta}, E) = \frac{\partial K_0}{\partial p_{\theta}}$$
 ; $T(p_{\theta}, E) = \frac{\partial K_0}{\partial E}$ Eq. 3

 $T(p_{\theta},E)$ is the toroidal transit time of circulating particles and it decreases with energy. $\iota(p_{\theta},E)$ is the drift rotational transform. Particles circulating around the torus having initial values θ_0,t_0,p_0,E_0 will change these values to θ_1,t_1,p_1,E_1 after one toroidal transit $\phi \longrightarrow \phi+2\pi$. The map describing this transformation has the generating function

$$S = S(p_1, \theta_0, E_1, t_0) = p_1 \theta_0 + E_1 t_0 + K_0(E_1, p_1) + S_1(p_1, \theta_0, E_1, t_0)$$
 Eq. 4

The four mapping equations are (Eq. 5)

$$E_{0} = E_{1} + \frac{\partial S_{1}}{\partial t_{0}} \; ; \quad t_{1} = t_{0} + T\Big(E_{1}, p_{1}\Big) + \frac{\partial S_{1}}{\partial E_{1}} \; ; \quad p_{0} = p_{1} + \frac{\partial S_{1}}{\partial \theta_{0}} \; ; \quad \theta_{1} = \theta_{0} + \iota\Big(p_{1}, E_{1}\Big) + \frac{\partial S_{1}}{\partial p_{1}} \; ; \quad \theta_{2} = \rho_{1} + \frac{\partial S_{2}}{\partial \rho_{1}} \; ; \quad \theta_{3} = \theta_{1} + \iota\Big(p_{1}, E_{2}\Big) + \frac{\partial S_{3}}{\partial \rho_{3}} \; ; \quad \theta_{3} = \theta_{1} + \iota\Big(p_{1}, E_{2}\Big) + \frac{\partial S_{3}}{\partial \rho_{3}} \; ; \quad \theta_{4} = \theta_{1} + \iota\Big(p_{1}, E_{2}\Big) + \frac{\partial S_{3}}{\partial \rho_{3}} \; ; \quad \theta_{5} = \rho_{5} + \iota\Big(p_{1}, E_{2}\Big) + \frac{\partial S_{3}}{\partial \rho_{3}} \; ; \quad \theta_{7} = \rho_{7} + \iota\Big(p_{1}, E_{2}\Big) + \frac{\partial S_{3}}{\partial \rho_{3}} \; ; \quad \theta_{8} = \rho_{8} + \iota\Big(p_{1}, E_{1}\Big) + \frac{\partial S_{3}}{\partial \rho_{1}} \; ; \quad \theta_{8} = \rho_{8} + \iota\Big(p_{1}, E_{1}\Big) + \frac{\partial S_{3}}{\partial \rho_{1}} \; ; \quad \theta_{8} = \rho_{8} + \iota\Big(p_{1}, E_{1}\Big) + \frac{\partial S_{3}}{\partial \rho_{1}} \; ; \quad \theta_{8} = \rho_{8} + \iota\Big(p_{1}, E_{1}\Big) + \frac{\partial S_{3}}{\partial \rho_{1}} \; ; \quad \theta_{8} = \rho_{8} + \iota\Big(p_{1}, E_{1}\Big) + \frac{\partial S_{3}}{\partial \rho_{1}} \; ; \quad \theta_{8} = \rho_{8} + \iota\Big(p_{1}, E_{1}\Big) + \frac{\partial S_{3}}{\partial \rho_{1}} \; ; \quad \theta_{8} = \rho_{8} + \iota\Big(p_{1}, E_{1}\Big) + \frac{\partial S_{3}}{\partial \rho_{1}} \; ; \quad \theta_{8} = \rho_{8} + \iota\Big(p_{1}, E_{1}\Big) + \frac{\partial S_{3}}{\partial \rho_{1}} \; ; \quad \theta_{8} = \rho_{8} + \iota\Big(p_{1}, E_{1}\Big) + \frac{\partial S_{3}}{\partial \rho_{1}} \; ; \quad \theta_{8} = \rho_{8} + \iota\Big(p_{1}, E_{1}\Big) + \frac{\partial S_{3}}{\partial \rho_{1}} \; ; \quad \theta_{8} = \rho_{8} + \iota\Big(p_{1}, E_{1}\Big) + \frac{\partial S_{3}}{\partial \rho_{1}} \; ; \quad \theta_{8} = \rho_{8} + \iota\Big(p_{1}, E_{1}\Big) + \frac{\partial S_{3}}{\partial \rho_{1}} \; ; \quad \theta_{8} = \rho_{8} + \iota\Big(p_{1}, E_{1}\Big) + \frac{\partial S_{3}}{\partial \rho_{1}} \; ; \quad \theta_{8} = \rho_{8} + \iota\Big(p_{1}, E_{1}\Big) + \frac{\partial S_{3}}{\partial \rho_{1}} \; ; \quad \theta_{8} = \rho_{8} + \iota\Big(p_{1}, E_{1}\Big) + \frac{\partial S_{3}}{\partial \rho_{1}} \; ; \quad \theta_{8} = \rho_{8} + \iota\Big(p_{1}, E_{1}\Big) + \frac{\partial S_{3}}{\partial \rho_{1}} \; ; \quad \theta_{8} = \rho_{8} + \iota\Big(p_{1}, E_{1}\Big) + \frac{\partial S_{3}}{\partial \rho_{1}} \; ; \quad \theta_{8} = \rho_{8} + \iota\Big(p_{1}, E_{1}\Big) + \frac{\partial S_{3}}{\partial \rho_{1}} \; ; \quad \theta_{8} = \rho_{8} + \iota\Big(p_{1}, E_{1}\Big) + \frac{\partial S_{3}}{\partial \rho_{1}} \; ; \quad \theta_{8} = \rho_{8} + \iota\Big(p_{1}, E_{1}\Big) + \frac{\partial S_{3}}{\partial \rho_{1}} \; ; \quad \theta_{8} = \rho_{8} + \iota\Big(p_{1}, E_{1}\Big) + \frac{\partial S_{3}}{\partial \rho_{1}} \; ; \quad \theta_{8} = \rho_{8} + \iota\Big(p_{1}, E_{1}\Big) + \frac{\partial S_{3}}{\partial \rho_{1}} \; ; \quad \theta_{8} = \rho_{8} + \iota\Big(p_{1}, E_{1}\Big) + \frac{\partial S_{3}}{\partial \rho_{1}} \; ; \quad \theta_{8} = \rho_{8} + \iota\Big(p_{1}, E_{1}\Big) + \frac{\partial S_{3}}{\partial \rho_{1}} \;$$

The perturbation S_1 is uniquely determined by the perturbation of the Hamiltonian K_1 . K_1 describes all possible drift wave spectra in a plasma. Instead of specifying K_1 one can as well specify the action S_1 and study the generic behaviour of transit particles under the influence of S_1 . Equations 5 are two couples area-preserving maps which in case of time-independent perturbations are reduced to one area-preserving map. The general form of the perturbation

$$S_1 = \text{Re} \sum_{l} S_{mnl}(p, E) \exp[im\varphi + in\theta + il\omega t]$$
 Eq. 6

 ω is the fundamental frequency of the drift wave. The relation between S₁ and K₁ is discussed in ref. 3. Due to the periodicity of the perturbation resonances occur and the resonance condition is $n \iota(p,E) + l\omega T(p,E) - m = 0$. For given numbers m,n,l this is a curve in the p-E-plane and all curves together represent the Arnold web. Without time-dependent perturbations (ωT =0) resonance only occurs on rational drift surfaces and enhanced radial losses can only arise if island overlap leads to a strong stochastisation of the particle orbits. Any time-dependent perturbation, however, can lead to a migration of the particles along the lines of the Arnold web and to radial loss of the particles.

3. Helias configurations

In Helias configurations like Wendelstein 7-X the magnetic shear is very small and we approximate the drift rotational transform by the magnetic transform. Furthermore, we adopt a simple model of the toroidal transit time, which is inversely proportional to the squre root of the energy. The rotational transform varies between 0.83 in the center and 1.0 at the boundary. Islands of drift surfaces — like in magnetic surfaces — arise at $\iota = 5/6$ and $\iota = 5/5$.

$$n\left(\iota_0 + \delta \iota p^3\right) + l\omega T\left(E_0\right)\sqrt{\frac{E_0}{E}} - m = 0$$
 Eq. 7

δι is a measure of the shear, which is small in Helias configurations.

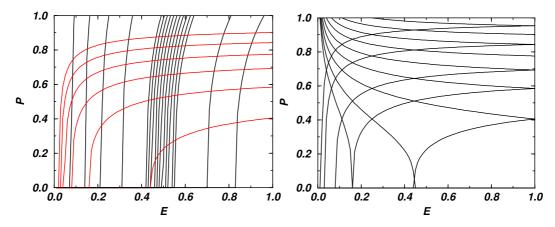
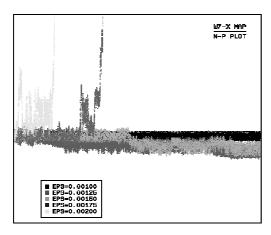


Fig. 1: Left: Densely covered Arnold web with a number of resonances that may lead to rapid losses for mode numbers around n=50, m=150 and $l\omega T=90$. Steep lines in the Arnold web can also originate from several low mode number perturbations (e.g. n=1, m=2, $l\omega T=1$). Right: Arnold web for W7-X with mode numbers n=50, $l\omega T=\pm 1$ and various numbers m=40...48.

Numerical computations of the drift-wave turbulence in Helias configurations exhibit a rich spectrum of mode numbers. The next figures show the Arnold web for high mode numbers, which are of relevance in drift wave turbulence. For numerical calculations we write eq.8 in the form

$$S_1 = \sum_{lmn} K_{lmn}^1 \left(p, E \right) \frac{m}{b} \left[\cos(\alpha) - \cos(\alpha + b) \right]$$
 Eq. 8

 $a = n\theta_0 + l\omega t_0$ and $b = (-m+nt+l\omega T)$ and K^1_{lmn} as in eq.3. An additional mode number dependent amplitude factor f(m,n,l,p) represents spectral and radial mode structure variations. The resulting mapping equations are written in dimensionless form, with e.g. energies normalized to thermal energy and frequencies $\omega -> \omega a_0/c_s$. All free parameters are determined by linear or nonlinear drift wave calculations in Helias geometry. Typical linear mode numbers in [7] are $m \approx n \approx 50$ and frequencies in the order of the diamagnetic frequency of electrons. For simplicity we here assume a radially constant mode amplitude and no static radial electric field. Particles are launched at specified radial position and initial energy and circulate N times around the torus. For several sets of parameters (see captions) we show results of our test particle simulations with regard to confinement time and time-dependent radial excursion (N-p plot) in the following figures.



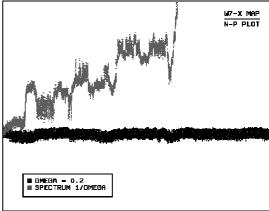


Fig. 2: Left: Test particle excursions for different values of electric potential perturbation amplitude (EPS): An increase of EPS leads to an overlap of the trajectory with a resonance in the Arnold web and rapid radial losses. All particles are launched at P_0 =0.5, ω = 0.5 and E = 1.0. Right: Comparison of test particle excursions $p_{\theta}(N)$ for a constant frequency electric potential perturbation $\omega a_0/c_s$ = 0.2 (black), and with a 1/ ω type spectrum (as found in drift-Alfvén turbulence simulations and also experiments in the plasma edge of stellarators) of the same integrated amplitude (red). The presence of a whole spectrum of frequencies leads to a higher probability of hitting an Arnold web resonance. The abcissa is the number of toroidal transits N.

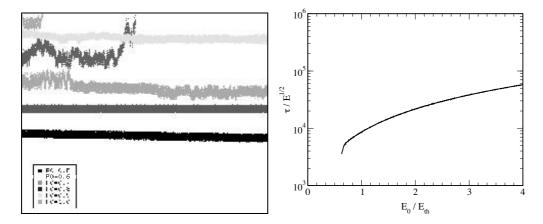


Fig. 3: Left: The influence of ergodization around static magnetic 5/6 islands on trajectories can be seen by launching the test particles from different radial positions with a drift wave perturbation amplitude that is sub-critical for most of the start positions P_0 . ($\omega a_0/cs=0.5$). Right: Dependence of the test particle confinement time $\tau(E_0)$ in the W7-X map on initial energy E_0 . Test particle orbits are launched at half radius and are subject to an electrostatic perturbation with intensity $q\delta\Phi/E_{th}=0.1$. The perturbation frequency $\omega a_0/c_s=0.65$ has been obtained by linear eigenmode calculation in Wendelstein 7-X geometry.

4. Summary

Numerical calculations have been carried out for test particletransport in a low-shear stellarator magnetic field with time-dependent electrostatic drift wave perturbations. Trajectories obtained by mapping techniques are not self-consistent, in the sense that particle motion does not act back on the perturbed electric potential. However, they allow for investigation of long time scale test particle behaviour, when the perturbation is prescribed by predetermined linear or nonlinear drift modes. Time-dependent perturbations together with variable energy lead to enhanced diffusion described by migration on an Arnold web. Our simulations have assumed radially local mode structure, and global drift waves together with equilibrium radial electric field will be treated in a future publication.

^[1] A.J. Lichtenberg, *Phys. Fluids* B**4**, (10) Oct. 1992, 3132

^[2] J.M. Kwon, W. Horton, P. Zhu, P.J. Morrison, H.B. Park, D.I. Choi, Phys. Plasmas, Vol. 7, No.4 (2000) 1169

^[3] H. Wobig, D. Pfirsch, IPP-report IPPIII/245

^[4] J. Nührenberg and R. Zille, *Phys. Lett.* A **114**, 129 (1986).

^[5] B.D. Scott, *Plasma Phys. Control. Fusion* **39**, 471 (1997)

^[6] J.D. Meiss, R.D. Hazeltine, Phys. Fluids B2, (1990) 2563

^[7] A. Kendl and H. Wobig, *Phys. Plasmas* **6**, 4714 (1999)